PHYSICAL REVIEW A **86**, 013412 (2012)

Molecular Siegert states in an electric field

Linda Hamonou,[1] Toru Morishita,[1] and Oleg I. Tolstikhin[2]
[1]*Department of Engineering Science, The University of Electro-Communications, 1-5-1 Chofu-ga-oka, Chofu-shi, Tokyo 182-8585, Japan*
[2]*National Research Center "Kurchatov Institute", Kurchatov Square 1, Moscow 123182, Russia*

(Received 1 May 2012; published 16 July 2012)

The Siegert states of atoms and molecules in a static electric field are the solutions of the stationary Schrödinger equation satisfying the regularity and outgoing-wave boundary conditions. Recently, an efficient method for calculating Siegert states in the single-active-electron approximation based on the adiabatic expansion in parabolic coordinates was proposed [P. A Batishchev *et al.*, Phys. Rev. A **82**, 023416 (2010); O. I. Tolstikhin *et al.*, *ibid.* **84**, 053423 (2011)]. So far, this method has been implemented only for axially symmetric potentials, which corresponds to atoms and linear molecules aligned along the field. In the present work, we extend its implementation to a general class of soft-core molecular potentials. This makes it possible to calculate the Siegert eigenvalue $E = \mathcal{E} - i\Gamma/2$ defining the energy $\mathcal{E}$ and ionization rate Γ of the corresponding state as functions of the electric field for arbitrarily oriented polyatomic molecules. The method is illustrated by calculations for the $1s\sigma$ and $2p\pi$ states of H_2^+. Comparison of the results with the predictions of perturbation theory for $\mathcal{E}$ and weak-field asymptotic theory for Γ is discussed.

DOI: 10.1103/PhysRevA.86.013412

PACS number(s): 32.60.+i, 33.80.Rv, 42.50.Hz

I. INTRODUCTION

The ionization of atoms and molecules by a static electric field is one of the fundamental problems in quantum mechanics. A new wave of interest in this problem over the past two decades has been motivated by the appearance of intense low-frequency laser pulses. It is clear that for a fixed intensity and sufficiently low frequency, the ionization in a time-dependent laser field $\mathbf{F}(t)$ should proceed as that in a static field $\mathbf{F}$ equal to the momentary value of $\mathbf{F}(t)$. This corresponds to the adiabatic regime. The adiabatic theory [1,2] establishes a condition under which the adiabatic approximation holds and provides a description of the dynamics of ionization in a laser field in terms of characteristics of the ionization process in a static field. We note that, in contrast to a common belief, the adiabatic regime does not coincide with the tunneling regime of the Keldysh theory [3,4]; more details are given in Ref. [2]. The ionization of atoms and molecules by laser pulses is the first step for a variety of strong-field-induced rescattering phenomena of current interest, such as the generation of high-order harmonics [5,6] and high-energy photoelectrons [6,7]. An accurate quantitative description of this step is obviously required. The present study continues our previous work [8,9] on the theory of field ionization in the adiabatic regime.

Recently, we have initiated the Siegert-state approach to the theory of ionization of atoms and molecules by a static electric field [8]. The main object in this approach is the solution to the stationary Schrödinger equation for the active electron (we restrict our consideration to the single-active-electron approximation) satisfying the regularity and outgoing-wave boundary conditions and coinciding with a given unperturbed bound state in the absence of a field. Solutions to this eigenvalue problem are called Siegert states (SSs) in an electric field. The SS eigenvalue $E = \mathcal{E} - i\Gamma/2$ is complex and defines the energy $\mathcal{E}$ and ionization rate Γ of the state. The asymptotic behavior of the SS eigenfunction defines the transverse momentum distribution (TMD) of the ionized electrons. These are the characteristics of the SS needed for the adiabatic theory [1,2]. To calculate SSs, we have proposed the method of adiabatic expansion in parabolic coordinates. In Ref. [8], this method was formulated and implemented for axially symmetric potentials, which corresponds to atoms and linear molecules aligned along the field. The accuracy and efficiency of this method were demonstrated by calculations of energies, ionization rates, and TMDs for hydrogen and rare-gas atoms in a wide range of fields, from tunneling to the overbarrier regime. In Ref. [9], the formulation of the method was extended to general potentials, which corresponds to molecules arbitrarily oriented with respect to the field. In addition to its computational efficiency, the method of adiabatic expansion in parabolic coordinates provides a theoretical framework suitable for analytical treatment of the problem in the weak-field limit. In Ref. [9], the weak-field asymptotic theory of tunneling ionization of atoms (spherically symmetric potentials) developed in classical studies [10–15] was generalized to molecules (arbitrary potentials). This theory was applied to the analysis of tunneling ionization of a number of the simplest linear molecules [16] and to the extraction of electron-ion differential scattering cross sections from experimentally obtained rescattering photoelectron spectra for C_2H_4 [17]. While the weak-field asymptotic theory is very useful in the region of its applicability, it fails quantitatively for stronger fields F approaching a boundary F_c between tunneling and overbarrier regimes. Meanwhile, the maximum field amplitude in currently available laser pulses far exceeds F_c. In this case, an accurate description of the ionization process can be obtained only by means of numerical calculations. Therefore in the present study we return to the computational aspect of the approach initiated in Ref. [8] and extend the implementation of the method of adiabatic expansion in parabolic coordinates to general molecular potentials.

Our computational procedure generalizes the one developed in Ref. [8] for axially symmetric potentials by coupling different azimuthal components of the SS eigenfunction. It is based on the slow-variable discretization (SVD) method [18] in combination with the R-matrix propagation technique [19]. In the present implementation, the adiabatic channel functions are constructed using a global discrete variable representation (DVR) basis [20–22]. Such an approach encounters difficulties in treating more than one Coulomb singularity of the potential at the positions of nuclei but is very efficient for *soft-core* potentials obtained by smoothing out these singularities. Apart from the smoothing, no other restrictions on the shape of the potential are imposed. Thus our procedure enables one to consider arbitrarily oriented polyatomic molecules. In the present work, we discuss only the calculation of the SS eigenvalues. The field and orientation dependence of the ionization rates of molecules are of great interest for current applications. The discussion of TMDs is postponed to future studies.

The paper is organized as follows. In Sec. II, we summarize basic equations of the method of adiabatic expansion in parabolic coordinates. In Sec. III, we describe our computational procedure. In Sec. IV, we present some illustrative numerical results for a soft-core model of the simplest molecule—the hydrogen molecular ion H_2^+. The energies $\mathcal{E}$ and ionization rates Γ of the $1s\sigma$ and $2p\pi$ states of H_2^+ are calculated and presented as functions of the electric field and the angle between the molecular axis and the field. A comparison of the results with the predictions of perturbation theory [10] for $\mathcal{E}$ and weak-field asymptotic theory [9] for Γ is discussed. The results are also compared with other accurate time-independent calculations for H_2^+ available in the literature [23–25]. Section V concludes the paper, indicating a direction for future studies.

II. THEORY: ADIABATIC EXPANSION IN PARABOLIC COORDINATES

A detailed account of the method of adiabatic expansion in parabolic coordinates for calculating SSs in an electric field is given in Ref. [8], for potentials that are axially symmetric about the direction of the field, and in [9], for the general case of potentials without any symmetry. Here we summarize basic equations needed for the present study. The Schrödinger equation for an active electron interacting with a molecular potential $V(\mathbf{r})$ and a static electric field $\mathbf{F} = F\mathbf{e}_z$, $F \geqslant 0$, in the laboratory frame reads (atomic units are used throughout the paper)

$$\left[-\tfrac{1}{2}\Delta + V(\mathbf{r}) + Fz - E\right]\psi(\mathbf{r}) = 0. \tag{1}$$

The electronic coordinate $\mathbf{r}$ is measured from the center of mass of the molecule [9]. The potential $V(\mathbf{r})$ describes the interaction with nuclei and other electrons in the single-active-electron approximation. It is assumed that this interaction is originally represented by a potential in a molecular frame $V_{\mathrm{MF}}(\mathbf{r}')$, where $\mathbf{r}'$ is the coordinate in the molecular frame. Then $V(\mathbf{r}) = V_{\mathrm{MF}}(\hat{R}\,\mathbf{r})$, where $\hat{R}$ is a rotation from the laboratory to the molecular frame. Thus the potential in Eq. (1) implicitly depends on the orientation of the molecule; a change in the orientation is implemented by rotating the molecular frame with respect to the laboratory frame, while the direction of the electric field $\mathbf{F}$ is kept fixed. We solve Eq. (1) using parabolic coordinates defined by [10]:

$$\xi = r + z, \quad 0 \leqslant \xi < \infty, \tag{2a}$$

$$\eta = r - z, \quad 0 \leqslant \eta < \infty, \tag{2b}$$

$$\varphi = \arctan\frac{y}{x}, \quad 0 \leqslant \varphi < 2\pi. \tag{2c}$$

In these coordinates, Eq. (1) can be presented in the form

$$\left[\frac{\partial}{\partial\eta}\eta\frac{\partial}{\partial\eta} + \mathcal{B}(\eta) + \frac{E\eta}{2} + \frac{F\eta^2}{4}\right]\psi(\xi,\eta,\varphi) = 0, \tag{3}$$

where

$$\mathcal{B}(\eta) = \frac{\partial}{\partial\xi}\xi\frac{\partial}{\partial\xi} + \frac{1}{4}\left(\frac{1}{\xi} + \frac{1}{\eta}\right)\frac{\partial^2}{\partial\varphi^2} - \frac{\xi+\eta}{2}V(\xi,\eta,\varphi) + \frac{E\xi}{2} - \frac{F\xi^2}{4} \tag{4}$$

is an operator acting on functions of ξ and φ and depending on η as a parameter. The eigenvalues $\beta_\nu(\eta)$ and eigenfunctions $\Phi_\nu(\xi,\varphi;\eta)$ of $\mathcal{B}(\eta)$ are the solutions of the adiabatic eigenvalue problem,

$$[\mathcal{B}(\eta) - \beta_\nu(\eta)]\,\Phi_\nu(\xi,\varphi;\eta) = 0, \tag{5a}$$

$$\Phi_\nu(\xi = 0,\varphi;\eta) < \infty, \quad \Phi_\nu(\xi \to \infty,\varphi;\eta) = 0, \tag{5b}$$

$$\Phi_\nu(\xi,\varphi + 2\pi;\eta) = \Phi_\nu(\xi,\varphi;\eta). \tag{5c}$$

They also depend on η as a parameter. For any η, the eigenfunctions are orthogonal and normalized by

$$\langle\Phi_\nu|\Phi_\mu\rangle \equiv \int_0^\infty\int_0^{2\pi}\Phi_\nu(\xi,\varphi;\eta)\Phi_\mu(\xi,\varphi;\eta)\,d\xi\,d\varphi = \delta_{\nu\mu}. \tag{6}$$

For the numerical treatment, it is convenient to introduce a cutoff parameter η_c and divide the whole space into an inner, $\eta < \eta_c$, and an outer, $\eta > \eta_c$, region. We assume that

$$V(\xi,\eta,\varphi)|_{\eta>\eta_c} = -\frac{Z}{r}, \quad r = \frac{\xi+\eta}{2}, \tag{7}$$

thus retaining only the monopole Coulomb tail of the potential in the outer region. We note that the dipole term in the asymptotics of $V(\mathbf{r})$ can always be eliminated by shifting the coordinate origin in Eq. (1) and appropriately changing the energy [9]; the effect of higher multipoles should be reduced by increasing η_c. Substituting Eq. (7) into Eq. (4), one can see that the eigenfunctions $\Phi_\nu(\xi,\varphi;\eta)$ cease to depend on η for $\eta > \eta_c$. Let us introduce the asymptotic basis defined by

$$\Phi_\nu(\xi,\varphi;\eta)|_{\eta>\eta_c} = \Phi_\nu(\xi,\varphi). \tag{8}$$

Equation (5a) allows the separation of variables in the outer region, so the functions $\Phi_\nu(\xi,\varphi)$ can be constructed more explicitly. Let $\beta_{n_\xi|m|}$, $\phi_{n_\xi|m|}(\xi)$, and $\Phi_{n_\xi m}(\xi,\varphi)$ be defined by

$$\left[\frac{d}{d\xi}\xi\frac{d}{d\xi} - \frac{m^2}{4\xi} + Z + \frac{E\xi}{2} - \frac{F\xi^2}{4} - \beta_{n_\xi|m|}\right]\phi_{n_\xi|m|}(\xi) = 0, \tag{9a}$$

$$\phi_{n_\xi|m|}(\xi)|_{\xi\to0} \propto \xi^{|m|/2}, \quad \phi_{n_\xi|m|}(\xi)|_{\xi\to\infty} = 0, \tag{9b}$$

$$\int_0^\infty \phi_{n_\xi|m|}(\xi)\phi_{n'_\xi|m|}(\xi)\,d\xi = \delta_{n_\xi n'_\xi}, \tag{9c}$$

and

$$\Phi_{n_\xi m}(\xi,\varphi) = \phi_{n_\xi |m|}(\xi)\,\frac{e^{im\varphi}}{\sqrt{2\pi}}. \tag{10}$$

Here $m = 0,\pm1,\pm2,\dots$ is the azimuthal quantum number and $n_\xi = 0,1,2,\dots$ enumerates the different solutions to Eq. (9a) for a given value of $|m|$. Then the asymptotic basis is given by

$$\Phi_\nu(\xi,\varphi) = \begin{cases} \Phi_{n_\xi 0}(\xi,\varphi), & m=0,\\ c_{|m|\lambda}\Phi_{n_\xi |m|}(\xi,\varphi) + c^*_{|m|\lambda}\Phi_{n_\xi -|m|}(\xi,\varphi), & m\neq 0.\end{cases} \tag{11}$$

The coefficients $c_{|m|\lambda}$ can be obtained by diagonalizing the matrix of $rV(\mathbf{r})$ in the subspace of two degenerate states $\Phi_{n_\xi \pm m}(\xi,\varphi)$ at $\eta=\eta_c$, and $\lambda = 1,2$ enumerates the eigenvectors of this matrix. The adiabatic eigenvalues in the outer region are given by

$$\beta_\nu(\eta)|_{\eta>\eta_c} = \beta_{n_\xi |m|} - \frac{m^2}{4\eta}. \tag{12}$$

Equations (11) and (12) show that in the outer region the adiabatic channels can be enumerated by the multi-index

$$\nu = (n_\xi, |m|, \lambda). \tag{13}$$

By continuity, this classification of the solutions to Eqs. (5) by asymptotic quantum numbers can be applied to all values of η.

Having thus defined the adiabatic basis, we seek the solution of Eq. (3) in the form of the adiabatic expansion,

$$\psi(\xi,\eta,\varphi) = \sum_\nu f_\nu(\eta)\Phi_\nu(\xi,\varphi;\eta). \tag{14}$$

Substituting this into Eq. (3), one obtains a set of coupled ordinary differential equations defining the coefficient functions $f_\nu(\eta)$,

$$\begin{aligned}&\left[\frac{d}{d\eta}\eta\frac{d}{d\eta} + \beta_\nu(\eta) + \frac{E\eta}{2} + \frac{F\eta^2}{4}\right] f_\nu(\eta)\\ &\quad + \sum_\mu \left[P_{\nu\mu}(\eta)\left(2\eta\frac{d}{d\eta}+1\right) + \eta Q_{\nu\mu}(\eta)\right] f_\mu(\eta) = 0,\end{aligned} \tag{15}$$

where the matrices

$$P_{\nu\mu}(\eta) = \left\langle \Phi_\nu \middle| \frac{\partial\Phi_\mu}{\partial\eta}\right\rangle, \quad Q_{\nu\mu}(\eta) = \left\langle \Phi_\nu \middle| \frac{\partial^2\Phi_\mu}{\partial\eta^2}\right\rangle \tag{16}$$

represent nonadiabatic couplings. As follows from Eq. (8), these matrices vanish in the outer region, so the different channels become decoupled for $\eta > \eta_c$ and Eq. (15) takes the form

$$\left[\frac{d^2}{d\eta^2} + \frac{1-m^2}{4\eta^2} + \frac{\beta_{n_\xi |m|}}{\eta} + \frac{E}{2} + \frac{F\eta}{4}\right]\eta^{1/2} f_\nu(\eta) = 0. \tag{17}$$

For a nonzero electric field, $F > 0$, the outgoing-wave solution to this equation satisfies

$$f_\nu(\eta)|_{\eta\to\infty} = \frac{2^{1/2} f_\nu}{F^{1/4}\eta^{3/4}} \exp\left[\frac{iF^{1/2}\eta^{3/2}}{3} + \frac{iE\eta^{1/2}}{F^{1/2}}\right]. \tag{18}$$

Equations (15) must be solved subject to the regularity boundary conditions at $\eta = 0$ and the outgoing-wave boundary conditions, (18), at $\eta\to\infty$. This is an eigenvalue problem; its solutions are called SSs in an electric field [8,9]. For any potential $V(\mathbf{r})$, there exist infinitely many SSs. In the present work, we are interested only in *tunneling states* which originate from bound states in the absence of the field. Let E_0 and $\psi_0(\mathbf{r})$ be the energy and wave function of a selected bound state. We discuss the solution to Eq. (1) satisfying

$$E|_{F\to0} = E_0, \quad \psi(\mathbf{r})|_{F\to0} = \psi_0(\mathbf{r}). \tag{19}$$

It should be noted that there exists another type of SSs called *static-field-induced states*, which do not have counterparts for $F = 0$ [1,26]. The eigenvalue E is generally complex. Presented in the form

$$E = \mathcal{E} - \frac{i}{2}\Gamma, \tag{20}$$

it defines the energy $\mathcal{E}$ and ionization rate Γ of the selected state. In this paper, we restrict ourselves to the description of a method for calculating the SS eigenvalue E. The coefficients f_ν in Eq. (18) determine the TMD of the ionized electrons [8,9]. Their calculation requires knowledge of the properly normalized SS eigenfunction $\psi(\mathbf{r})$. The discussion of TMDs for molecules is postponed to future studies.

III. COMPUTATIONAL PROCEDURE

To use SSs as a theoretical tool for various applications in strong-field physics, one must be able to efficiently solve Eq. (3) for general molecular potentials. We are not aware of any other approaches to this challenging problem, so we believe that it is worthwhile to give some details of the present computational procedure implementing the approach summarized in the previous section. This procedure generalizes the one developed in Ref. [8] for axially symmetric potentials by accounting for a coupling between the components of the wave function corresponding to different values of the azimuthal quantum number m. It is based on the SVD method [18] in combination with the R-matrix propagation technique [19] and, in this respect, is similar to a procedure used earlier in the theory of atom-diatom chemical reactions [27,28] and the three-body Coulomb problem [29–34]. Another essential technical element of this procedure is the DVR [20–22]. All necessary details on constructing DVRs associated with different types of classical orthogonal polynomials can be found in Ref. [32].

A. Adiabatic eigenvalue problem

We first discuss the solution of the adiabatic eigenvalue problem (5). For axially symmetric potentials, the azimuthal quantum number m is conserved. Then, for a given m, the adiabatic channel functions behave as $\Phi_\nu(\xi,\varphi;\eta)\propto\xi^{|m|/2}$ at $\xi\to0$. Such functions can be expanded in the DVR basis constructed from the generalized Laguerre polynomials $L_n^{(|m|)}(s\xi)$ [8]. In the general case, however, $\Phi_\nu(\xi,\varphi;\eta)$ contains integer as well as half-integer powers of ξ for $\xi\to0$, which cannot be represented by a single DVR basis with a fixed m. To resolve this difficulty we introduce a new variable x, defined by

$$x = (s\xi)^{1/2}. \tag{21}$$

The scaling factor s serves to adjust our basis in x to the region of localization of the main adiabatic channels contributing to Eq. (14) and thus accelerate convergence. Its optimal value for each potential and state is to be chosen empirically; in the present calculations we used $s \sim \sqrt{2|E|}$. In terms of the new variable Eq. (5a) reads

$$\left\{ s\frac{\partial}{\partial x}x\frac{\partial}{\partial x} + \left(\frac{s}{x}+\frac{x}{\eta}\right)\frac{\partial^2}{\partial\varphi^2} - x[2(\xi+\eta)V(\xi,\eta,\varphi) - 2E\xi + F\xi^2 + 4\beta_\nu(\eta)]\right\}\Phi_\nu(\xi,\varphi;\eta) = 0. \tag{22}$$

The solutions to this equation contain only integer powers of x at $x \to 0$, which was the goal of transformation (21). They can be expanded in the direct product of two independent basis sets in x and φ,

$$\Phi_\nu(\xi,\varphi;\eta) = \sum_{i_1 i_2} a^\nu_{i_1 i_2}(\eta)\pi^{(\xi)}_{i_1}(x)\pi^{(\varphi)}_{i_2}(\varphi). \tag{23}$$

Here $\pi^{(\xi)}_i(x)$ is the DVR basis constructed from ordinary Laguerre polynomials $L_n(x) = L^{(0)}_n(x)$ [32] satisfying the regularity and asymptotic boundary conditions (5b), and $\pi^{(\varphi)}_i(\varphi)$ is that based on the Chebyshev quadrature and constructed from sine and cosine functions [35] satisfying the periodic boundary conditions (5c). Substituting Eq. (23) into Eq. (22), we obtain the algebraic eigenvalue problem

$$\begin{aligned}\sum_{j_1 j_2}\left[sK^{(\xi)}_{i_1 j_1}\delta_{i_2 j_2} + \left(\frac{s}{x_{i_1}}+\frac{x_{i_1}}{\eta}\right)\delta_{i_1 j_1}K^{(\varphi)}_{i_2 j_2}\right]a^\nu_{j_1 j_2}(\eta)\\ + x_{i_1}\big[2\big(\xi_{i_1}+\eta\big)V\big(\xi_{i_1},\eta,\varphi_{i_2}\big) - 2E\xi_{i_1} + F\xi^2_{i_1}\\ + 4\beta_\nu(\eta)\big]a^\nu_{i_1 i_2}(\eta) = 0,\end{aligned} \tag{24}$$

where x_i and φ_i are the Laguerre and Chebyshev quadrature points, respectively, and $\xi_i = x_i^2/s$. The kinetic energy matrices for the motion in x and φ are given by

$$K^{(\xi)}_{ij} = \int_0^\infty \frac{d\pi^{(\xi)}_i(x)}{dx}\,x\,\frac{d\pi^{(\xi)}_j(x)}{dx}\,dx, \tag{25a}$$

$$K^{(\varphi)}_{ij} = \int_0^{2\pi} \frac{d\pi^{(\varphi)}_i(\varphi)}{d\varphi}\,\frac{d\pi^{(\varphi)}_j(\varphi)}{d\varphi}\,d\varphi. \tag{25b}$$

They can be calculated analytically by the methods described in Refs. [32,35]. Equation (24) is solved by standard linear algebra routines. Thus the eigenvalues $\beta_\nu(\eta)$ and the coefficients $a^\nu_{i_1 i_2}(\eta)$ in Eq. (23) can be obtained for the different adiabatic channels at any point η. Substituting Eq. (23) into Eq. (6), the orthonormalization condition takes the form

$$\frac{2}{s}\sum_{i_1 i_2} x_{i_1} a^\nu_{i_1 i_2}(\eta)a^\mu_{i_1 i_2}(\eta) = \delta_{\nu\mu}, \tag{26}$$

which follows from the orthogonality and normalization of the DVR basis functions [32,35].

The approach to solving a two-dimensional eigenvalue problem (5) described above uses a global DVR basis and therefore works well only for sufficiently smooth potentials. This is the case for soft-core molecular potentials obtained by smoothing out Coulomb singularities at the nuclei. In this case, the DVR basis indeed ensures rapid convergence and high accuracy of the results. In principle, it is possible to account for the Coulomb singularities by switching to some local basis, like finite elements. Such an approach, however, would require a very flexible numerical grid, since the positions of the nuclei in terms of the coordinates ξ and φ depend on the internuclear configuration and orientation of the molecule, and its implementation for arbitrary molecules does not seem to be straightforward.

B. Slow-variable discretization and *R*-matrix propagation

Here we discuss the solution of Eq. (3) in the inner region $0 \leqslant \eta \leqslant \eta_c$. This region is divided into N sectors,

$$0 = \bar\eta_0 < \bar\eta_1 < \cdots < \bar\eta_N = \eta_c. \tag{27}$$

Consider the kth sector, $\bar\eta_- \equiv \bar\eta_{k-1} \leqslant \eta \leqslant \bar\eta_k \equiv \bar\eta_+$. The R-matrix basis in this sector is defined by

$$\left[\frac{\partial}{\partial\eta}\eta\frac{\partial}{\partial\eta} - \mathcal{L} + \mathcal{B}(\eta) + \frac{\bar E_n\eta}{2} + \frac{F\eta^2}{4}\right]\bar\psi_n(\xi,\eta,\varphi) = 0, \tag{28}$$

where $\mathcal{L}$ is the Bloch operator [36],

$$\mathcal{L} = \eta\,[\delta(\eta-\bar\eta_+) - \delta(\eta-\bar\eta_-)]\,\frac{\partial}{\partial\eta}. \tag{29}$$

The different solutions of Eq. (28) are orthonormal with weight η,

$$\int_{\bar\eta_-}^{\bar\eta_+}\langle\bar\psi_n(\xi,\eta,\varphi)|\bar\psi_m(\xi,\eta,\varphi)\rangle\eta\,d\eta = \delta_{nm}. \tag{30}$$

We solve Eq. (28) by the SVD method [18]. To this end, we introduce a new variable y by substituting

$$\eta = \eta(y), \quad \eta(\pm 1) = \bar\eta_\pm. \tag{31}$$

The function $\eta(y)$ should be monotonic, so that its inverse maps the sector under consideration onto the interval $-1 \leqslant y \leqslant 1$; the explicit form of $\eta(y)$ is given below. The solutions to Eq. (28) are sought in the form of the SVD expansion [18],

$$\bar\psi_n(\xi,\eta,\varphi) = \sum_{i\nu} c^n_{i\nu}\pi^{(\eta)}_i(y)\Phi_\nu(\xi,\varphi;\eta_i). \tag{32}$$

Here $\pi^{(\eta)}_i(y)$ is the DVR basis constructed from the Legendre polynomials [32] and $\eta_i = \eta(y_i)$, where y_i are the Legendre quadrature points. Substituting Eq. (32) into Eq. (28), we obtain the SVD eigenvalue problem

$$\sum_{j\mu} K^{(\eta)}_{ij}O_{i\nu,j\mu}c^n_{j\mu} - \eta'_i\left[\beta_\nu(\eta_i) + \frac{\bar E_n\eta_i}{2} + \frac{F\eta_i^2}{4}\right]c^n_{i\nu} = 0, \tag{33}$$

where $K^{(\eta)}_{ij}$ is the kinetic energy matrix,

$$K^{(\eta)}_{ij} = \int_{-1}^{1}\frac{d\pi^{(\eta)}_i(y)}{dy}\,\frac{\eta(y)}{\eta'(y)}\,\frac{d\pi^{(\eta)}_j(y)}{dy}\,dy, \tag{34}$$

$O_{i\nu,j\mu}$ is the overlap matrix of the adiabatic bases at the different quadrature points,

$$O_{i\nu,j\mu} = \langle\Phi_\nu(\xi,\varphi;\eta_i)|\Phi_\mu(\xi,\varphi;\eta_j)\rangle, \tag{35}$$

and $\eta'_i = \eta'(y_i)$. Comparing the approaches based on expansions (14) and (32), it is seen that the SVD method enables one to avoid solving tedious differential equations with nonadiabatic couplings (15) and calculating the matrices (16). Instead, one needs to calculate the overlap matrix (35), which can be easily done using the quadrature associated with the DVR expansion (23), and to solve an algebraic eigenvalue problem (33). Thus we obtain the R-matrix eigenvalues $\bar{E}_n$ and eigenfunctions $\bar{\psi}_n(\xi,\eta,\varphi)$ for the sector. Substituting Eq. (32) into Eq. (30), the orthonormalization condition takes the form

$$\sum_{i\nu} \eta'_i \eta_i c^n_{i\nu} c^m_{i\nu} = \delta_{nm}, \tag{36}$$

which follows from the properties of the DVR basis functions [32] and Eq. (6).

Let us return to the function $\eta(y)$ defining the variable transformation (31). This transformation has different forms in the first and further sectors. For axially symmetric potentials, solutions to Eq. (28) with a given azimuthal quantum number m behave as $\bar{\psi}_n(\xi,\eta,\varphi) \propto \eta^{|m|/2}$ at $\eta \to 0$. Substituting $\eta(y) = \bar{\eta}_1(1+y)/2$, such functions can be expanded in terms of the DVR basis constructed from the Jacobi polynomials $P_n^{(0,|m|)}(y)$ [8]. In the general case, however, $\bar{\psi}_n(\xi,\eta,\varphi)$ contains integer as well as half-integer powers of η for $\eta \to 0$. This difficulty is similar to that discussed in Sec. III A, so its remedy is known. The function $\eta(y)$ in the first sector $0 \leqslant \eta \leqslant \bar{\eta}_1$ is defined by

$$\eta(y) = \frac{\bar{\eta}_1}{4}(1+y)^2. \tag{37}$$

The solutions to Eq. (28) contain only integer powers of $(1 + y)$ at $y \to -1$, which corresponds to $\eta \to 0$, and hence can be expanded in the DVR basis constructed from the Legendre polynomials $P_n(y) = P_n^{(0,0)}(y)$, as in Eq. (32). We note that nonlinear variable transformations similar to Eqs. (21) and (31) with $\eta(y)$ given by Eq. (37), whose goal is to get rid of half-integer powers of the corresponding variables when there is a coupling between different azimuthal components of the wave function, have recently been used in calculations of elastic scattering on two-center Coulomb potentials [37]. In sectors with $k \geqslant 2$, the difficulty discussed above does not arise, and we use a linear transformation defined by

$$\eta(y) = \tfrac{1}{2}\left[(\bar{\eta}_+ + \bar{\eta}_-) + (\bar{\eta}_+ - \bar{\eta}_-)y\right]. \tag{38}$$

For both functions (37) and (38), matrix (34) can be calculated analytically using the formulas given in Ref. [32].

The R matrix $\mathbf{R}(\eta;E)$ for the solutions to Eq. (3) with respect to the adiabatic channels is defined by [38]

$$\begin{aligned}\langle \Phi_\nu(\xi,\varphi;\eta)|\psi(\xi,\eta,\varphi)\rangle \\ = \sum_\mu R_{\nu\mu}(\eta;E)\left\langle \Phi_\nu(\xi,\varphi;\eta)\middle|\frac{\partial\psi(\xi,\eta,\varphi)}{\partial\eta}\right\rangle.\end{aligned} \tag{39}$$

Having the solutions to Eq. (28), the matrix $\mathbf{R}(\eta;E)$ can be propagated through the sector. The propagation is accomplished by means of the equation [19]

$$\mathbf{R}(\bar{\eta}_\pm;E) = \pm\mathcal{R}^{(\pm,\pm)} - \mathcal{R}^{(\pm,\mp)}[\mathbf{R}(\bar{\eta}_\mp;E) \pm \mathcal{R}^{(\mp,\mp)}]^{-1}\mathcal{R}^{(\mp,\pm)}, \tag{40}$$

where the matrices $\mathcal{R}^{(\pm,\pm)}$ are given by

$$\mathcal{R}^{(\pm,\pm)}_{\nu\mu} = 2\sum_n \frac{\bar{f}^n_\nu(\bar{\eta}_\pm)\bar{f}^n_\mu(\bar{\eta}_\pm)}{\bar{E}_n - E}. \tag{41}$$

Here

$$\begin{aligned}\bar{f}^n_\nu(\bar{\eta}_\pm) &= \bar{\eta}_\pm^{1/2}\langle\Phi_\nu(\xi,\varphi;\bar{\eta}_\pm)|\bar{\psi}_n(\xi,\bar{\eta}_\pm,\varphi)\rangle \\ &= \bar{\eta}_\pm^{1/2}\sum_{j\mu} c^n_{j\mu}\pi^{(\eta)}_j(\pm 1)O^\pm_{\nu,j\mu}\end{aligned} \tag{42}$$

are the surface amplitudes of the R-matrix eigenfunctions, and

$$O^\pm_{\nu,j\mu} = \langle\Phi_\nu(\xi,\varphi;\bar{\eta}_\pm)|\Phi_\mu(\xi,\varphi;\eta_j)\rangle \tag{43}$$

are the surface overlap matrices. Solving Eq. (28) for each sector in the inner region and applying Eq. (40), one can propagate $\mathbf{R}(\eta,E)$ between any two boundary points $\bar{\eta}_k$. The procedure described above enables one to do this for any given energy E and field F.

C. Outgoing-wave boundary conditions

In the outer region $\eta > \eta_c$, we need to solve Eq. (17) subject to the outgoing-wave boundary condition (18). The solution $f_\nu(\eta)$ rapidly oscillates with an exponentially growing amplitude as $\eta \to \infty$ along the real axis. In addition, it approaches its asymptotic form very slowly; the relative error of Eq. (18) decays as $1/\eta$. These two circumstances make it very difficult to achieve a high accuracy in the calculations staying on the real η axis. An efficient solution of this problem was proposed in Ref. [8]. The idea is to deform the real interval $[\eta_c,\infty)$ into a contour in the complex η plane along which the solution decays. This is possible because the coefficients in Eq. (17) are known analytically. We solve Eq. (17) along a semiclassical steepest descent contour $\mathcal{C}$ (a Stokes line) defined by [8]

$$\mathrm{Re}\int_{\eta_c}^{\eta}\left[\frac{1-m^2}{4\eta'^2} + \frac{\beta_{n_\xi|m|}}{\eta'} + \frac{E}{2} + \frac{F\eta'}{4}\right]^{1/2} d\eta' = 0 \to \eta \in \mathcal{C}. \tag{44}$$

This contour begins at $\eta = \eta_c$ and runs to infinity in the upper half of the complex η plane parallel to the ray $\arg\eta = \pi/3$. The outgoing-wave solution to Eq. (17) exponentially decays as η goes to infinity along this contour, thus Eq. (18) amounts to zero asymptotic boundary condition for $f_\nu(\eta)$ on $\mathcal{C}$. We start from a point $\eta_\infty \in \mathcal{C}$, for which the integral in Eq. (44) has a sufficiently large value, and propagate the solution of Eq. (17) along $\mathcal{C}$ inward to η_c by the fourth-order Runge-Kutta method [39]. Because of a well-known numerical instability caused by the finite accuracy of the calculations, independently of the initial conditions for $f_\nu(\eta)$, only the exponentially growing solution survives in the propagation. This is the solution we need, the one satisfying the outgoing-wave boundary condition (18). We note that this procedure works also for $F = 0$, even though the asymptotic form of the solution in this case differs from Eq. (18). Thus one can obtain $f_\nu(\eta)$ up to a constant factor, which is sufficient to find the SS eigenvalue E. The result of the calculations in the outer region is a set of the ratios

$$r_\nu(E) = \left.\frac{f_\nu(\eta)}{f'_\nu(\eta)}\right|_{\eta=\eta_c} \tag{45}$$

for all adiabatic channels included in Eq. (32).

D. The matching condition

For the solutions to Eq. (3) regular at $\eta = 0$, we have

$$R_{\nu\mu}(0; E) = 0. \tag{46}$$

For the solutions satisfying outgoing-wave boundary conditions at $\eta \to \infty$, we have

$$R_{\nu\mu}(\eta_c; E) = r_\nu(E)\delta_{\nu\mu}, \tag{47}$$

where $r_\nu(E)$ is given by Eq. (45). Equations (46) and (47) provide the boundary conditions for R-matrix propagation. Starting from Eq. (46) and propagating $\mathbf{R}(\eta; E)$ through k sectors to the right, we obtain $\mathbf{R}_{\text{left}}(\bar{\eta}_k; E)$. On the other hand, starting from Eq. (47) and propagating $\mathbf{R}(\eta; E)$ through $N - k$ sectors to the left, we obtain $\mathbf{R}_{\text{right}}(\bar{\eta}_k; E)$. The requirement of continuity of the solution to Eq. (3) and its derivative with respect to η at $\eta = \bar{\eta}_k$ leads to the matching condition,

$$\det[\mathbf{R}_{\text{left}}(\bar{\eta}_k; E) - \mathbf{R}_{\text{right}}(\bar{\eta}_k; E)] = 0. \tag{48}$$

The values of E for which this equation is satisfied are the SS eigenvalues. We solve Eq. (48) iteratively, starting from $F = 0$ and incrementing F by sufficiently small steps. For $F = 0$, we find the solution $E = E_0$ corresponding to the selected bound state; see Eqs. (19). The initial guess in this case is provided by the calculations discussed in Sec. IV A. At each next step in F, we seek the 0 of the smallest eigenvalue of the matrix in Eq. (48) closest to the solution E found at the previous step using the Newton method [39]. In this way, E can be continued to any generally complex value of F. We note that, apart from numerical errors and finiteness of the step in F, this procedure yields E as an *analytic* function of F. The corresponding SS is thus obtained as the *analytic continuation* of the selected bound state in F, which is essential for applications of SSs in the adiabatic theory [1,2].

Let us conclude this discussion of the computational procedure by specifying the typical values of the numerical parameters used in the calculations for H_2^+ reported below. We use 30 and 15 DVR basis functions in Eq. (23) for x and φ, respectively. The cutoff parameter is $\eta_c = 75$. The inner region is divided into $N = 150$ equal sectors, (27). In each sector, we use six DVR basis functions and 60 adiabatic channels in Eq. (32). The matching condition (48) is applied at $\bar{\eta}_k \sim 10$, where the unperturbed bound-state wave function $\psi_0(\mathbf{r})$ still has a large amplitude.

IV. WEAK-FIELD APPROXIMATIONS

For sufficiently small values of F, the energy $\mathcal{E}$ and ionization rate Γ of a tunneling SS defined by Eqs. (19) and (20) can be found using perturbation theory [10] and the recently developed weak-field asymptotic theory [9], respectively. It is instructive to compare the exact results obtained by solving Eq. (1) with the predictions of these weak-field approximations, to test the consistency and accuracy of the former and clarify the region of applicability of the latter. In this section, we give necessary details on the present implementation of the weak-field approximations.

Since in the illustrative calculations reported in Sec. V we consider H_2^+, here we restrict our treatment to nonpolar linear molecules. We choose a geometry in which the molecular axis z' lies in the xz plane of the laboratory frame. The orientation of the molecule is described by an angle β between its axis and the direction of the electric field coinciding with that of the laboratory z axis (see Fig. 1). Thus $\mathcal{E}$ and Γ for a given state are functions of F and β. The unperturbed bound-state wave function $\psi_0(\mathbf{r})$ is characterized by the projection of the electronic angular momentum onto the molecular axis, which is denoted M. We consider only states with $M = 0$ (σ states) and $|M| = 1$ (π states). The unperturbed energy E_0 for states with $M \neq 0$ does not depend on the sign of M. This degeneracy is removed by an arbitrarily weak field, provided that $\beta \neq 0$. The correct bound-state wave functions of the zeroth order are certain linear combinations of the two degenerate states [10]. One of them is even and the other is odd with respect to the reflection $y \to -y$. The even and odd states are indicated by superscripts $+$ and $-$, respectively. Nondegenerate σ states belong to the class of even states. The wave functions for even and odd π states are illustrated in Fig. 1.

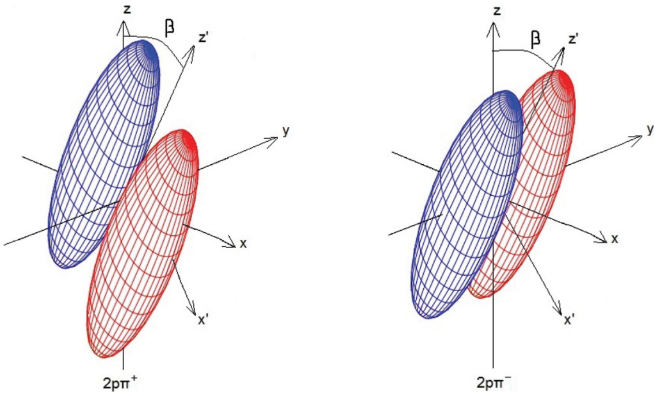

FIG. 1. (Color online) Illustration of the unperturbed wave functions of H_2^+ oriented under an angle β with respect to the direction of the field in even $2p\pi^+$ and odd $2p\pi^-$ states. Different colors correspond to different signs of the wave function.

A. Perturbation theory

As follows from the above discussion, the molecular frame is obtained by rotating the laboratory frame around its y axis by an angle β. Let $(x',y',z') \equiv (x_1',x_2',x_3')$ and (r',θ',φ') denote the Cartesian and spherical coordinates in the molecular frame, respectively, where $y' = y$ and $r' = r$. The static dipole polarizability tensor in the molecular frame is diagonal, $\alpha_{x_i'x_j'} = \alpha_{x_i'}\delta_{ij}$, where $\alpha_{x_i'}$ is the polarizability in the direction of the axis x_i'. Then the energy of the state satisfying Eqs. (19) in the second order of perturbation theory is given by [10]

$$\mathcal{E} = E_0 - \frac{F^2}{2}(\alpha_{x'}\sin^2\beta + \alpha_{z'}\cos^2\beta). \tag{49}$$

The polarizabilities $\alpha_{x_i'}$ can be expressed in terms of the eigenvalues $E_{n|M|}$ and eigenfunctions ψ_{nM} of the unperturbed Hamiltonian [10],

$$\alpha_{x_i'} = 2\sum_{nM\neq 0}\frac{\langle\psi_0|x_i'|\psi_{nM}\rangle\langle\psi_{nM}|x_i'|\psi_0\rangle}{E_{n|M|} - E_0}, \tag{50}$$

where n is a set of quantum numbers which, together with M, identify the state and the summation runs over the complete set of states excluding the unperturbed one indicated by the subscript 0. The eigenfunctions ψ_{nM} in the molecular frame have the form

$$\psi_{nM}(r',\theta',\varphi') = f_n^{|M|}(r',\theta')\,\frac{e^{iM\varphi'}}{\sqrt{2\pi}}. \tag{51}$$

The matrix elements needed are then given by

$$\langle\psi_{n'M'}|x'|\psi_{nM}\rangle = \tfrac{1}{2}\big\langle f_{n'}^{|M'|}\big|r'\sin\theta'\big|f_n^{|M|}\big\rangle(\delta_{M'\,M+1}+\delta_{M'\,M-1}), \tag{52a}$$

$$\langle\psi_{n'M'}|z'|\psi_{nM}\rangle = \big\langle f_{n'}^{|M'|}\big|r'\cos\theta'\big|f_n^{|M|}\big\rangle\delta_{M'M}. \tag{52b}$$

If the unperturbed state is a σ state ψ_{n0}, we obtain

$$\alpha_{x'} = \sum_{n'}\frac{\big|\big\langle f_{n'}^{1}\big|r'\sin\theta'\big|f_n^{0}\big\rangle\big|^2}{E_{n'1}-E_{n0}}, \tag{53a}$$

$$\alpha_{z'} = 2\sum_{n'\neq n}\frac{\big|\big\langle f_{n'}^{0}\big|r'\cos\theta'\big|f_n^{0}\big\rangle\big|^2}{E_{n'0}-E_{n0}}. \tag{53b}$$

For unperturbed states with $M\neq 0$, the even $\psi_{n|M|}^{+}$ and odd $\psi_{n|M|}^{-}$ correct wave functions of the zeroth order are given by

$$\psi_{n|M|}^{+} = \frac{1}{\sqrt{2}}(\psi_{n|M|}+\psi_{n\,-|M|}) = f_n^{|M|}(r',\theta')\frac{\cos|M|\varphi'}{\sqrt{\pi}}, \tag{54a}$$

$$\psi_{n|M|}^{-} = \frac{1}{i\sqrt{2}}(\psi_{n|M|}-\psi_{n\,-|M|}) = f_n^{|M|}(r',\theta')\frac{\sin|M|\varphi'}{\sqrt{\pi}}. \tag{54b}$$

For these states, the matrix elements needed are

$$\begin{aligned}\langle\psi_{n'M'}|x'|\psi_{n|M|}^{\pm}\rangle = {}& \frac{1}{2\sqrt{2}}\big\langle f_{n'}^{|M'|}\big|r'\sin\theta'\big|f_n^{|M|}\big\rangle(\delta_{M'\,M+1}\\ &+\delta_{M'\,M-1}\pm\delta_{M'\,-M+1}\pm\delta_{M'\,-M-1}),\end{aligned} \tag{55a}$$

$$\langle\psi_{n'M'}|z'|\psi_{n|M|}^{\pm}\rangle = \frac{1}{\sqrt{2}}\big\langle f_{n'}^{|M'|}\big|r'\cos\theta'\big|f_n^{|M|}\big\rangle(\delta_{M'\,M}\pm\delta_{M'\,-M}). \tag{55b}$$

In particular, for an even π state ψ_{n1}^{+}, we obtain

$$\alpha_{x'} = \sum_{n'}\frac{\big|\big\langle f_{n'}^{0}\big|r'\sin\theta'\big|f_n^{1}\big\rangle\big|^2}{E_{n'0}-E_{n1}} + \frac{1}{2}\sum_{n'}\frac{\big|\big\langle f_{n'}^{2}\big|r'\sin\theta'\big|f_n^{1}\big\rangle\big|^2}{E_{n'2}-E_{n1}}, \tag{56a}$$

$$\alpha_{z'} = 2\sum_{n'\neq n}\frac{\big|\big\langle f_{n'}^{1}\big|r'\cos\theta'\big|f_n^{1}\big\rangle\big|^2}{E_{n'1}-E_{n1}}. \tag{56b}$$

Similarly, for an odd π state ψ_{n1}^{-}, we find

$$\alpha_{x'} = \frac{1}{2}\sum_{n'}\frac{\big|\big\langle f_{n'}^{2}\big|r'\sin\theta'\big|f_n^{1}\big\rangle\big|^2}{E_{n'2}-E_{n1}}, \tag{57a}$$

$$\alpha_{z'} = 2\sum_{n'\neq n}\frac{\big|\big\langle f_{n'}^{1}\big|r'\cos\theta'\big|f_n^{1}\big\rangle\big|^2}{E_{n'1}-E_{n1}}. \tag{57b}$$

In the calculations for H_2^+ reported below, a complete set of the eigenvalues $E_{n|M|}$ and eigenfunctions $f_n^{|M|}(r',\theta')$ is obtained by solving Eq. (1) for $F=0$ with zero-derivative boundary conditions on a sphere of sufficiently large radius. We use a single-center expansion in the molecular frame and diagonalize the unperturbed Hamiltonian in the direct product of two DVR basis sets in r' and θ' constructed from the Legendre polynomials [32]. All the matrix elements are calculated using the Legendre quadrature. The polarizabilities $\alpha_{x'}$ and $\alpha_{z'}$ are evaluated by summing over all states in Eqs. (53), (56), and (57), including discretized continuum states for which $E_{n|M|}>0$. The radius of the sphere used in the calculations is 20, which is found to be large enough to obtain converged results in all the cases considered.

B. Asymptotic theory

The weak-field asymptotic theory of tunneling ionization of molecules was developed in Ref. [9]. Recently, it was applied to the analysis of tunneling ionization of a number of the simplest polar and nonpolar linear molecules [16,17]. According to this theory, the asymptotics of the ionization rate Γ for $F\to 0$ is given by a sum of partial rates for ionization into different channels defined by Eqs. (9) and (10) and labeled by parabolic quantum numbers (n_ξ,m). The leading-order term in the asymptotics is determined by the dominant channel with the minimum values of n_ξ and $|m|$. For linear molecules, the dominant channel is $(n_\xi=0,m)$, where $m=0$ and 1 for even and odd unperturbed states, respectively. For a nonpolar linear molecule in a state satisfying Eqs. (19), the ionization rate is given by

$$\Gamma_{\rm as} = (2-\delta_{m0})|g_{0m}(\beta)|^2 W_{0m}(F)[1+O(F)], \tag{58}$$

where

$$\begin{aligned}g_{0m}(\beta) = {}& \sqrt{\frac{\varkappa^{|m|+1}}{|m|!}}\,\eta^{1+|m|/2-Z/\varkappa}e^{\varkappa\eta/2}\\ &\times\int_0^\infty\int_0^{2\pi}\xi^{|m|/2}\,e^{-\varkappa\xi/2-im\varphi}\,\psi_0(\mathbf{r})\,\frac{d\xi\,d\varphi}{\sqrt{2\pi}}\bigg|_{\eta\to\infty}\end{aligned} \tag{59}$$

and

$$W_{0m}(F) = \frac{\varkappa}{2}\left(\frac{4\varkappa^2}{F}\right)^{2Z/\varkappa-|m|-1}\exp\left(-\frac{2\varkappa^3}{3F}\right). \tag{60}$$

Here $\varkappa=\sqrt{2|E_0|}$ and Z is the asymptotic charge defined by Eq. (7). The condition of applicability of Eq. (58) is [9]

$$F \ll F_c = \frac{\varkappa^4}{8|2Z-\varkappa(m+1)|}, \tag{61}$$

where the critical field F_c indicates a boundary between tunneling and overbarrier regimes of ionization estimated as the field for which the two turning points in Eq. (17) coalesce. This condition ensures that the correction term in Eq. (58) that is linear in F is much smaller than unity and, hence, the leading-order term dominates.

As follows from Eq. (58), in the leading-order approximation the ionization rate factorizes into two factors, one of which depends only on the orientation angle β and the other depends only on the field F. The dependence on the orientation is determined by a structure factor [16] which, for nonpolar molecules, coincides with $g_{0m}(\beta)$. According to Eq. (59), this characteristic should be extracted from the asymptotic tail of the unperturbed wave function $\psi_0(\mathbf{r})$ at $\eta \to \infty$; in the present calculations we used a procedure described in Ref. [16]. The field-dependent factor is given by a simple analytic function (60) which depends on the molecule and state only via the parameters $\varkappa$ and Z.

As stated above, the azimuthal quantum number of the dominant ionization channel for even and odd unperturbed states is $m = 0$ and 1, respectively. This is true for all values of β except for some special orientations, if any, for which the integral in Eq. (59) for the dominant channel turns 0. For example, for the even $1s\sigma$ state of H_2^+ to be considered below, the dominant channel is $m = 0$ for all orientation angles β, because $g_{00}(\beta)$ never turns 0. Similarly for the odd $2p\pi^-$ state, the dominant channel is $m = 1$ for all values of β, because $g_{01}(\beta)$ never goes through 0. But for the even $2p\pi^+$ state, $g_{00}(\beta)$ vanishes at $\beta = 0$. For this state at not too small values of β, the dominant channel is $m = 0$. However, as β decreases, the contributions to the ionization rate from channels with $m = 0$ and $m = 1$ become comparable at $\beta \sim \beta_c$ and then the channel $m = 1$ becomes dominant. According to the weak-field asymptotic theory [9], for $\beta \lesssim \beta_c$ the contributions from both channels must be retained. The ionization rate in this case is given by [16],

$$\Gamma_{\beta \lesssim \beta_c} = \left(|g_{00}(\beta)|^2 + \frac{F}{2\varkappa^2} |g_{01}(\beta)|^2 \right) W_{00}(F)[1 + O(F)]. \tag{62}$$

The boundary β_c between the two regimes depends on F. Taking into account that for even π states $g_{00}(\beta \to 0) \propto \beta$, while $g_{01}(\beta \to 0) \neq 0$, one can see that $\beta_c \propto F^{1/2}$ as $F \to 0$. The interplay between the contributions to Γ from channels with $m = 0$ and $m = 1$ for even π states near $\beta = 0$ was discussed in Ref. [16]. For simplicity, in the present calculations we retain only the channel $m = 0$ in the asymptotic results for the $2p\pi^+$ state at $\beta \neq 0$, which is the dominant channel for $F \to 0$.

V. ILLUSTRATIVE RESULTS AND DISCUSSION

We have implemented the computational procedure described in Sec. III in a computer program. This program enables one to find the energy eigenvalue E for a selected SS by solving Eq. (1) for any sufficiently smooth molecular potential $V(\mathbf{r})$ and any orientation of the molecule. In this section we report some illustrative numerical results. We consider a soft-core model of the hydrogen molecular ion H_2^+ with the potential given by

$$V(\mathbf{r}) = -\frac{1}{\sqrt{\left|\mathbf{r} - \frac{\mathbf{R}}{2}\right|^2 + \epsilon}} - \frac{1}{\sqrt{\left|\mathbf{r} + \frac{\mathbf{R}}{2}\right|^2 + \epsilon}}. \tag{63}$$

Here $\mathbf{R} = (R \sin\beta, 0, R\cos\beta)$, R is the internuclear distance, β is the angle between the internuclear axis and the electric field (see Fig. 1), and ϵ is a softening parameter. Equation (63) complies with the definition of the potential in the laboratory frame given after Eq. (1) and implies that the laboratory and molecular frames coincide for $\beta = 0$. Most of the calculations discussed below were done with $R = 2$ and $\epsilon = 0.09$, but we also present some results for larger R and smaller ϵ. To illustrate the different symmetry cases, we consider SSs originating from the unperturbed ground state $1s\sigma$ with $M = 0$ and unperturbed even $2p\pi^+$ and odd $2p\pi^-$ excited states with $|M| = 1$. In Ref. [9], results for several model diatomic polar molecules described by a similar soft-core potential were reported. These results were obtained using the program developed in Ref. [8], and hence were restricted to the orientations with $\beta = 0^\circ$ and 180°, when the molecule is aligned along the field. In the present calculations, we examine the dependence of the energy $\mathcal{E}$ and ionization rate Γ on both the field F and the orientation angle β. The results obtained by solving Eq. (1), which for brevity are referred to as "exact" results, are compared with the weak-field approximations discussed in Sec. IV, namely, with the predictions of perturbation theory for $\mathcal{E}$ obtained from Eq. (49) and asymptotic theory for Γ obtained from Eq. (58).

A. The ground $1s\sigma$ state

We begin with the ground $1s\sigma$ state of the soft-core H_2^+ with $R = 2$ and $\epsilon = 0.09$. Our result for the field-free energy of this state is $E_0 = -0.962\,36$, which is slightly higher than the corresponding energy $-1.102\,634$ for the pure Coulomb potential with $\epsilon = 0$. Figure 2 presents the energy $\mathcal{E}$ and ionization rate Γ as functions of the electric field F for several representative orientation angles β. The exact results are compared with the results of the weak-field approximations. The static dipole polarizabilities in Eq. (49) in the present case are $\alpha_{x'} = 1.44$ and $\alpha_{z'} = 2.95$. The azimuthal quantum number of the dominant channel in Eq. (58) is $m = 0$. The critical field defined by Eq. (61) is $F_c \approx 0.18$

The top panels in Fig. 2 present the energy $\mathcal{E}$ of the state. For all orientations of the molecule, $\mathcal{E}$ decreases monotonically as the field F grows. In the tunneling regime, $F < F_c$, the energy decreases quadratically with F and its behavior agrees well with the predictions of perturbation theory. In the overbarrier regime, $F > F_c$, the energy continues to decrease almost linearly in the interval of F considered. A large deviation from the results of perturbation theory is seen in this region. The middle panels present the ionization rate Γ. For all orientations, Γ exponentially grows in the tunneling regime and continues to grow, but less rapidly, in the overbarrier regime. The asymptotic theory reproduces the behavior of Γ in the tunneling regime but overestimates its values at larger fields. The bottom panels present the ratio of the exact and asymptotic results for Γ. The usefulness of this ratio for gauging the performance of the weak-field asymptotic theory at a quantitative level was pointed out in Ref. [9]. It can be clearly seen that for all orientations the ratio $\Gamma/\Gamma_{\text{as}}$ approaches unity linearly as the field F decreases, as it should in accordance with Eq. (58). The curves are not continued to smaller F because of a fundamental limitation of the present numerical procedure in calculating very low ionization rates: the procedure yields a complex number E, and Γ is obtained from its imaginary part, so our calculations with double precision fail if $\Gamma/|E_0| \lesssim 10^{-10}$. The linear dependence of $\Gamma/\Gamma_{\text{as}}$ on F holds up to the onset F_c of the overbarrier regime. This dependence results from the correction term in square brackets in Eq. (58) that is linear in F. We note that the deviation of Γ from Γ_{as} is small only under condition (61); for

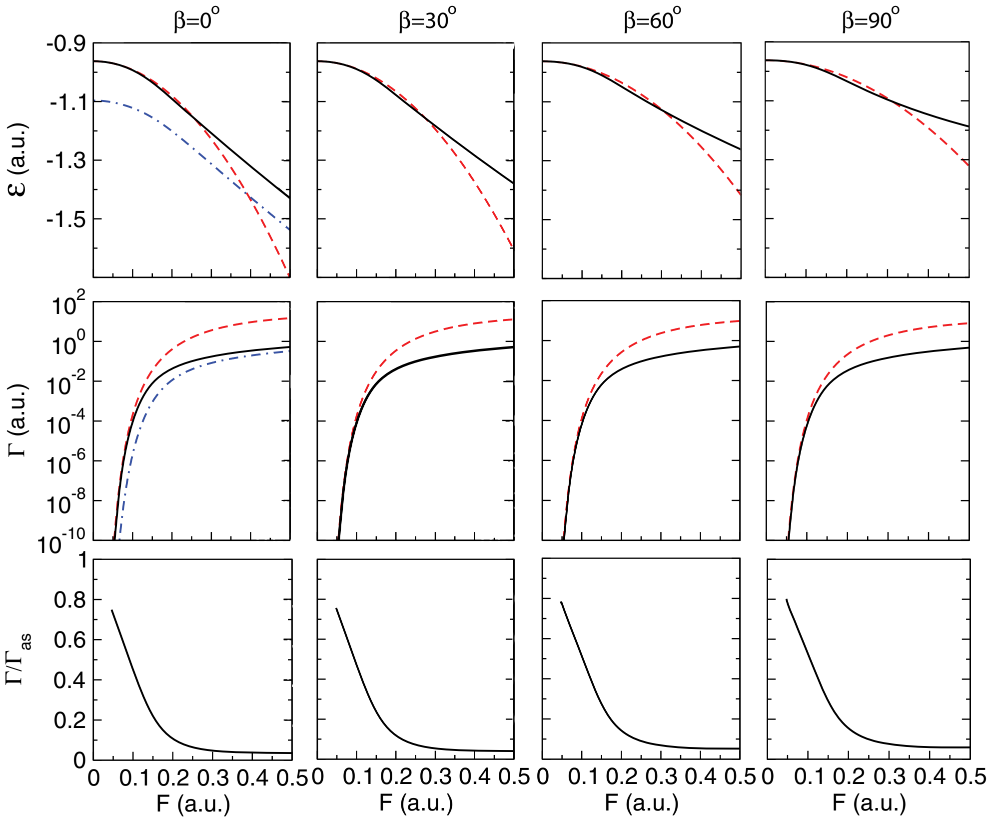

FIG. 2. (Color online) Energy $\mathcal{E}$ and ionization rate Γ for the $1s\sigma$ state of the soft-core H_2^+ with $R = 2$ and $\epsilon = 0.09$ as functions of the electric field F for four representative orientation angles β. Solid (black) lines for $\mathcal{E}$ and Γ: exact results. Dashed (red) lines: results of perturbation theory and asymptotic theory, respectively. Bottom panels: ratio of the exact to the asymptotic results for Γ. Dash-dotted (blue) lines for $\beta = 0°$: exact results for a sharper potential with $\epsilon = 0.0009$.

stronger fields, but still in the tunneling regime, the deviation becomes large. For example, for $F = 0.1$ the leading-order term in Eq. (58) overestimates the ionization rate by a factor of 2. The major part of this difference could be accounted for in the next order of the weak-field asymptotic theory [9] by calculating the correction term in Eq. (58). So far, this correction is available only for the hydrogen atom in an arbitrary state [15].

To illustrate the dependence of the results on the softening parameter in Eq. (63), we have performed calculations for the same state $1s\sigma$ and internuclear distance $R = 2$ as above, but for a sharper potential with $\epsilon = 0.0009$. The field-free energy in this case is $E_0 = -1.0963$, which is closer to the pure Coulomb case. To obtain the converged SS eigenvalue E for such a sharp potential, the density of DVR quadrature points near the nuclei in our numerical scheme must be essentially increased, so the calculations become more time-consuming. We restrict our calculations to the parallel geometry with $\beta = 0°$. The results are shown in the top and middle panels in the left column in Fig. 2. They look similar to the corresponding results for $\epsilon = 0.09$; the main difference is a shift of the energy $\mathcal{E}$ that is almost uniform in F which reproduces the shift of E_0.

Some accurate results for the energy and ionization rate of the $1s\sigma$ state of the pure Coulomb H_2^+ in a static electric field obtained by different methods are available in the literature [23–25]. Unfortunately, most of them are available only in graphical form; only several numerical values are given in Ref. [23]. To compare with these results, we have done calculations for $R = 6$ with $\epsilon = 0.0009$. Our value of the ionization rate for $F = 0.0533$ and $\beta = 0°$ is $\Gamma = 7.12 \times 10^{-6}$, which is slightly larger than the result $\Gamma = 5.69 \times 10^{-6}$ reported in [23]. Given the very rapid variation of Γ as a function of F in the tunneling regime, the two results essentially agree with each other. Their difference can be explained by a smaller value of the binding energy $|E_0|$ resulting from a nonzero value of the softening parameter ϵ in the present calculations.

Figure 3 presents the energy and ionization rate for the $1s\sigma$ state calculated with $R = 2$ and $\epsilon = 0.09$, as in Fig. 2, now as functions of the orientation angle β for two representative values of the field in tunneling ($F = 0.06$) and overbarrier ($F = 0.2$) regimes. In the left panel, the orientation dependence of the energy $\mathcal{E}$ is shown. Perturbation theory perfectly reproduces the exact results for the weaker field, which is expectable. But even for the stronger field in the overbarrier regime, the dependence of the exact $\mathcal{E}$ on β follows the prediction of Eq. (49), with a shift that is almost uniform in β. Thus perturbation theory works better than would be expected. Since in the present case $\alpha_{x'} < \alpha_{z'}$, the energy monotonically grows as β grows from 0° to 90° for a fixed F. In the right panel in Fig. 3, we plot the ionization rate Γ

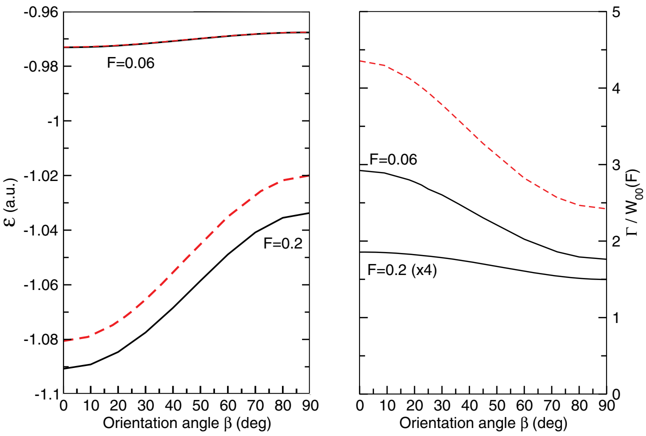

FIG. 3. (Color online) Energy $\mathcal{E}$ and normalized ionization rate $\Gamma/W_{00}(F)$ for the $1s\sigma$ state of H_2^+ with $R=2$ and $\epsilon=0.09$ as functions of the orientation angle β for two representative values of the field in tunneling ($F=0.06$) and overbarrier ($F=0.2$) regimes. Solid (black) lines: exact results. Note that for $F=0.2$ the results in the right panel are multiplied by 4. Dashed (red) lines for $\mathcal{E}$ and Γ: results of perturbation theory and asymptotic theory, respectively. For $F=0.06$, dashed and solid lines in the left panel cannot be distinguished at the scale of the figure.

divided by the field-dependent factor $W_{00}(F)$ for the dominant ionization channel defined by Eq. (60). According to the asymptotic theory, in the weak-field limit this ratio is given by the structure factor $|g_{00}(\beta)|^2$ plotted by the dashed (red) line. We note that this factor for the present soft-core model with $\epsilon=0.09$ is about 50% smaller than that for the pure Coulomb case [16]. For the weaker field, the shape of the orientation dependence of the exact results is indeed close to that of $|g_{00}(\beta)|^2$, although the magnitude differs by a factor of 0.7, which complies with the values of $\Gamma/\Gamma_{\text{as}}$ for $F=0.06$ shown in Fig. 2. This confirms the factorization of the leading-order term in Eq. (58) and indicates that the correction term only weakly depends on β. For the stronger field, the dependence of the ratio $\Gamma/W_{00}(F)$ on β becomes flatter and its magnitude essentially differs from the predictions of Eq. (58). In both cases, the ionization rate has a maximum at $\beta=0^\circ$; i.e., it is easier to ionize the molecule when it is parallel to the field.

B. Excited $2p\pi^{\pm}$ states

We now consider $2p\pi$ states of the soft-core H_2^+ with $R=2$ and $\epsilon=0.09$. As discussed in Sec. IV, for $F=0$ there are two degenerate $2p\pi$ states, one of which, $2p\pi^+$, is even and the other, $2p\pi^-$, is odd with respect to the reflection $y\to -y$. The wave functions of these states are illustrated in Fig. 1. Our result for the field-free energy of these states is $E_0=-0.4238$, which is, again, slightly higher than the corresponding energy $-0.428\,772$ for the pure Coulomb potential with $\epsilon=0$. The static dipole polarizability in the direction of the x' axis for the even and odd states is $\alpha_{x'}=46.83$ and 9.61, respectively; in both cases $\alpha_{z'}=11.70$. For the even state at $\beta\neq 0^\circ$, the azimuthal quantum number of the dominant ionization channel is $m=0$ and the critical field is $F_c\approx 0.029$. For the even state at $\beta=0^\circ$ and odd state at any β, the dominant channel is $m=1$, since the integral in Eq. (59) vanishes for $m=0$, and the critical field is $F_c\approx 0.042$.

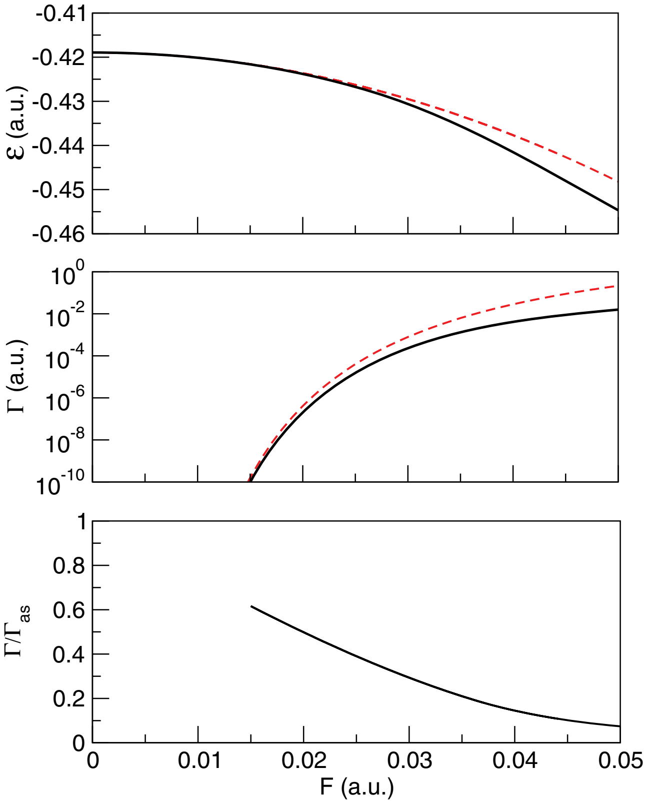

FIG. 4. (Color online) Energy $\mathcal{E}$ and ionization rate Γ for the $2p\pi^{\pm}$ states of H_2^+ with $R=2$ and $\epsilon=0.09$ as functions of the electric field F for $\beta=0^\circ$. Solid (black) lines for $\mathcal{E}$ and Γ: exact results. Dashed (red) lines: results of perturbation theory and asymptotic theory, respectively. Bottom panel: ratio of the exact to the asymptotic results for Γ.

Let us first discuss the parallel geometry with $\beta=0^\circ$. In this case, the states $2p\pi^+$ and $2p\pi^-$ are related by a rotation of 90° about the direction of the field (see Fig. 1). Since the SS eigenvalue is not affected by such a rotation, the states $2p\pi^{\pm}$ remain degenerate for all values of F. The energy and ionization rate of these states as functions of F for $\beta=0^\circ$ are shown in Fig. 4. The exact results are again compared with the weak-field approximations. The dominant channel in the present case is $m=1$ and the critical field is $F_c\approx 0.042$. The situation is similar to that for the $1s\sigma$ state discussed above. In the tunneling regime, $F<F_c$, perturbation theory works well and the ratio $\Gamma/\Gamma_{\text{as}}$ approaches unity linearly as F decreases. The curve in the bottom panel is not continued to smaller F for the reason explained above. In the overbarrier regime, $F>F_c$, we observe a large deviation of the exact results from the weak-field approximations, which is to be expected.

Figure 5 presents the results for the even $2p\pi^+$ state. The dependence of $\mathcal{E}$ and Γ on F for three representative nonzero values of β is shown. The dominant channel in this case is $m=0$ and the critical field is $F_c\approx 0.029$. The results for $\beta=60^\circ$ and 90° are similar to those shown in Figs. 2 and 4. The ratio $\Gamma/\Gamma_{\text{as}}$ exhibits a typical behavior: it approaches unity from below linearly as F decreases. However, the situation for $\beta=30^\circ$ in the bottom panel is different. In this case,

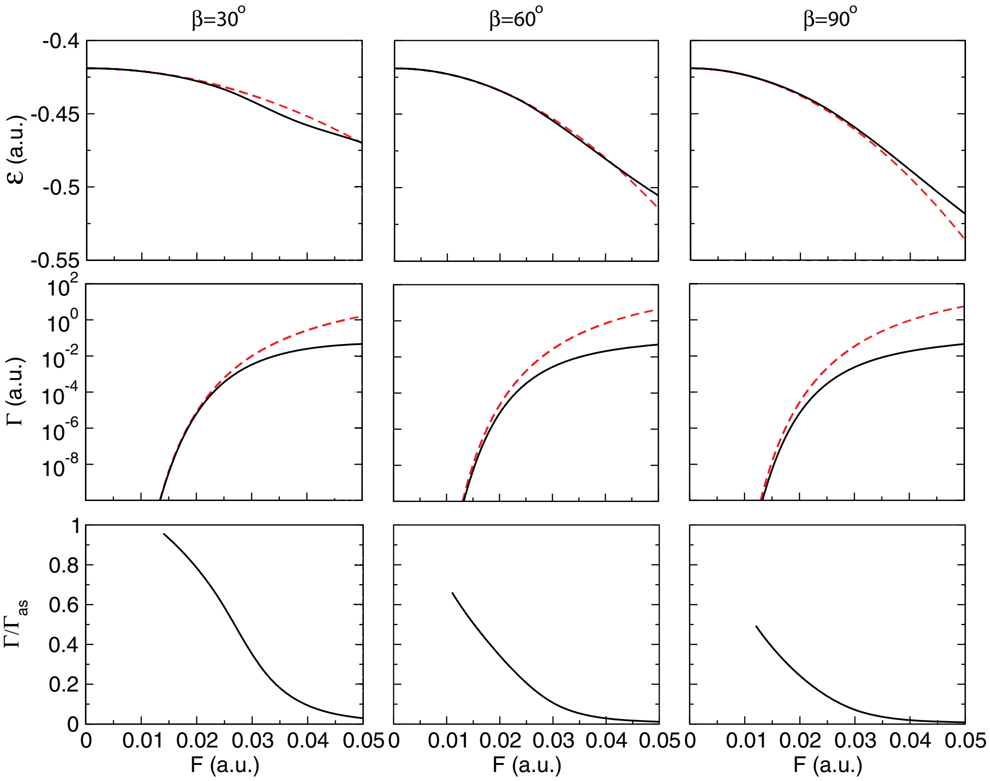

FIG. 5. (Color online) Energy $\mathcal{E}$ and ionization rate Γ for the even $2p\pi^+$ state of H_2^+ with $R = 2$ and $\epsilon = 0.09$ as functions of the electric field F for three representative orientation angles β. Solid (black) lines for $\mathcal{E}$ and Γ: exact results. Dashed (red) lines: results of perturbation theory and asymptotic theory, respectively. Bottom panels: ratio of the exact to the asymptotic results for Γ.

the ratio Γ/Γ_{as} apparently crosses unity somewhere near $F = 0.01$. Such a difference in the behavior of Γ/Γ_{as} is explained by the contribution from the channel with $m = 1$, which is not included in the present results for Γ_{as}. According to Eq. (62), the ratio Γ/Γ_{as} should reach a maximum and then approach unity, now from above, linearly in F as F decreases further. Unfortunately, we cannot check this prediction of the asymptotic theory because we cannot continue the curve to smaller F. The difference in the behavior of Γ/Γ_{as} should reveal itself for sufficiently small β, smaller than the maximum value of β_c in the tunneling regime. A similar behavior was found for the excited $2p\sigma$ state of HeH^{2+} (see Fig. 6 in Ref. [9]), although the reason in this case is different.

Figure 6 presents the energy and ionization rate for the same state $2p\pi^+$ as in Fig. 5, now as functions of the orientation angle β for several representative values of the field. In the left panel, we observe a good agreement with the results of perturbation theory. In contrast to the $1s\sigma$ state (see Fig. 3), the energy goes down as β grows for a fixed F, since in the present case $\alpha_{x'} < \alpha_{z'}$. A general trend shown in the right panel is that the ionization rate for $\beta = 90°$ is higher than that for $\beta = 0°$ for the same F. This agrees with the fact that the structure factor $|g_{00}(\beta)|^2$ shown by the dashed (black) line turns 0 at $\beta = 0°$. The exact ionization rates are not 0 at $\beta = 0°$, but their values are suppressed by an additional power of F in the field-dependent factor (60) for the dominant ionization channel $m = 1$ at $\beta = 0°$. A more careful inspection of Fig. 6 shows that the ionization rate has a maximum at some intermediate value of β. For example, for $F = 0.03$ the maximum is located at $\beta = 30°$. Its position moves toward larger β as F decreases and approaches 90° in the limit $F \to 0$, and simultaneously the value of $\Gamma/W_{00}(F)$ at the maximum grows, so the exact results approach the prediction of the asymptotic theory. We note that a maximum in the orientation dependence of Γ at smaller angles was also observed in the ionization yield produced by an intense short laser pulse obtained by solving the time-dependent Schrödinger equation [40].

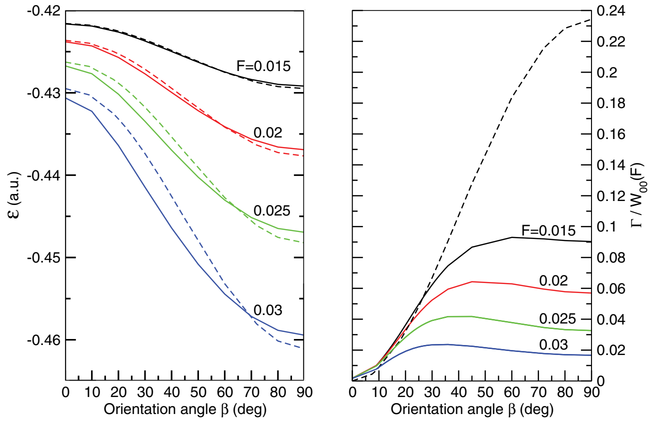

FIG. 6. (Color online) Energy $\mathcal{E}$ and normalized ionization rate $\Gamma/W_{00}(F)$ for the even $2p\pi^+$ state of H_2^+ with $R = 2$ and $\epsilon = 0.09$ as functions of the orientation angle β for four representative values of the field F. Solid lines: exact results. Dashed lines in left and right panels: results of perturbation theory and asymptotic theory, respectively.

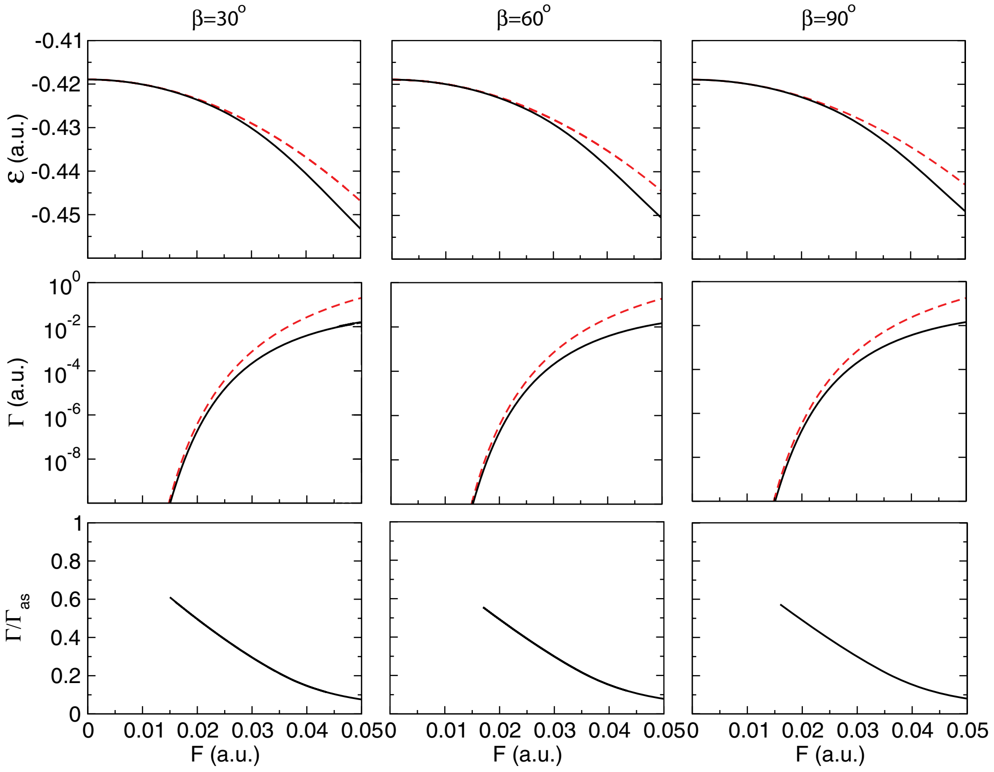

FIG. 7. (Color online) Same as Fig. 5, but for the odd $2p\pi^-$ state.

Figures 7 and 8 present similar results for the odd $2p\pi^-$ state. The dominant channel in this case is $m = 1$ and the critical field is $F_c \approx 0.042$. In the tunneling regime, $F < F_c$, the weak-field approximations work well again. The ratio $\Gamma/\Gamma_{\text{as}}$ approaches unity linearly as F decreases, since the channel $m = 1$ remains dominant for all values of β, including $\beta = 0^\circ$. We note that both the energy and the ionization rate only weakly depend on β for a fixed F, indicating that this state is almost axially symmetric about the y' axis.

Summarizing the discussion of these illustrative calculations, a good agreement between the exact and the approximate results in the deep tunneling regime $F \ll F_c$ confirms the consistency and accuracy of our method for solving Eq. (1). On the other hand, comparison of the results for $F \sim F_c$ clarifies the regions of applicability of perturbation theory for $\mathcal{E}$ and the weak-field asymptotic theory [9] for Γ.

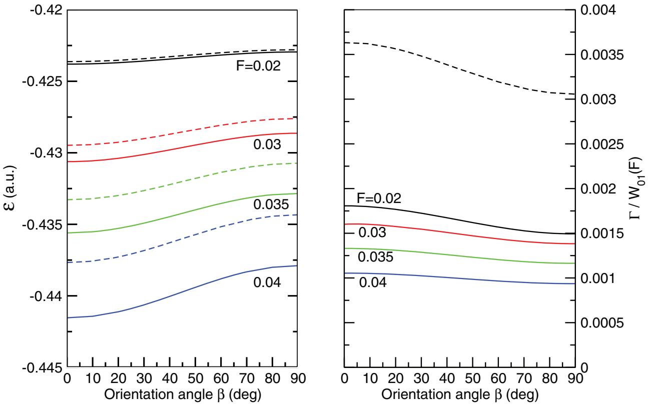

FIG. 8. (Color online) Same as Fig. 6, but for the odd $2p\pi^-$ state.

VI. CONCLUSION

The present study continues our previous work on the SS approach to the theory of ionization of atoms and molecules by a static electric field [8,9]. The implementation of the method of adiabatic expansion in parabolic coordinates is extended to a general class of soft-core potentials without any symmetry. This opens the possibility of calculating SSs in the single-active-electron approximation for polyatomic molecules that are arbitrarily oriented with respect to the field. The method is illustrated by calculations of energies and ionization rates of the $1s\sigma$ and $2p\pi$ states of H_2^+. While for weak fields in the deep tunneling regime $F \ll F_c$ the accurate results for $\mathcal{E}$ and Γ obtained by solving Eq. (1) agree well with the predictions of perturbation theory [10] and weak-field asymptotic theory [9], respectively, for stronger fields $F \gtrsim F_c$ the weak-field approximations fail and the present computational approach becomes indispensable. Since accurate field- and orientation-dependent ionization rates of molecules are of great interest for the analysis of current experiments, we believe that the present approach will find applications.

In this paper we have discussed only the calculation of the complex Siegert eigenvalue (20). For implementing the adiabatic theory [1,2] one also needs the properly normalized Siegert eigenfunction and the coefficients f_ν in Eq. (18) defining the amplitude of the TMD of the ionized electrons [8,9]. TheTMDs for atoms were calculated and discussed in Ref. [8]. An extension of the present computational method in this direction for molecules is a subject for future studies.

ACKNOWLEDGMENTS

This work was supported by a Grant-in-Aid for Scientific Research (C) from the Japan Society for the Promotion of Science. L.H. thanks the Japan Society for the Promotion of Science for funding this research project. O.I.T. thanks the Russian Foundation for Basic Research for support through Grant No. 11-02-00390-a. We wish to thank Professor S. Watanabe for providing excellent research environment throughout this work.

---

[1] O. I. Tolstikhin, T. Morishita, and S. Watanabe, Phys. Rev. A **81**, 033415 (2010).
[2] O. I. Tolstikhin and T. Morishita (in preparation).
[3] L. V. Keldysh, Zh. Eksp. Teor. Fiz. **47**, 1945 (1964) [Sov. Phys. JETP **20**, 1307 (1965)].
[4] V. S. Popov, Usp. Fiz. Nauk **174**, 921 (2004); Phys. Usp. **47**, 855 (2004).
[5] P. B. Corkum, Phys. Rev. Lett. **71**, 1994 (1993).
[6] T. Morishita, A.-T. Le, Z. Chen, and C. D. Lin, Phys. Rev. Lett. **100**, 013903 (2008).
[7] G. G. Paulus, W. Becker, W. Nicklich, and H. Walther, J. Phys. B **27**, L703 (1994).
[8] P. A. Batishchev, O. I. Tolstikhin, and T. Morishita, Phys. Rev. A **82**, 023416 (2010).
[9] O. I. Tolstikhin, T. Morishita, and L. B. Madsen, Phys. Rev. A **84**, 053423 (2011).
[10] L. D. Landau and E. M. Lifshitz, *Quantum Mechanics (Non-relativistic Theory)* (Pergamon Press, Oxford, 1977).
[11] Yu. N. Demkov and G. F. Drukarev, Zh. Eksp. Teor. Fiz. **47**, 918 (1964) [Sov. Phys. JETP **20**, 614 (1964)].
[12] B. M. Smirnov and M. I. Chibisov, Zh. Eksp. Teor. Fiz. **49**, 841 (1965) [Sov. Phys. JETP **22**, 585 (1966)].
[13] S. Yu. Slavyanov, Problemy Mat. Fiz. **4**, 125 (1970). [English translation: in *Topics in Mathematical Physics, Vol. 4* (Consultants Bureau, New Yorkn, 1971)].
[14] T. Yamabe, A. Tachibana, and H. J. Silverstone, Phys. Rev. A **16**, 877 (1977).
[15] R. J. Damburg and V. V. Kolosov, J. Phys. B **11**, 1921 (1978); **12**, 2637 (1979); Phys. Rev. A **16**, 877 (1977).
[16] L. B. Madsen, O. I. Tolstikhin, and T. Morishita, Phys. Rev. A **85**, 053404 (2012).
[17] C. Wang, M. Okunishi, R. R. Lucchese, T. Morishita, O. I. Tolstikhin, L. B. Madsen, K. Shimada, D. Ding, and K. Ueda, J. Phys. B **45**, 131001 (2012).
[18] O. I. Tolstikhin, S. Watanabe, and M. Matsuzawa, J. Phys. B **29**, L389 (1996).
[19] K. L. Baluja, P. G. Burke, and L. A. Morgan, Comput. Phys. Commun. **27**, 299 (1982).
[20] D. O. Harris, G. G. Engerholm, and W. D. Gwinn, J. Chem. Phys. **43**, 1515 (1965).
[21] A. S. Dickinson and P. R. Certain, J. Chem. Phys. **49**, 4209 (1968).
[22] J. C. Light, I. P. Hamilton, and J. V. Lill, J. Chem. Phys. **82**, 1400 (1985).
[23] Z. Mulyukov, M. Pont, and R. Shakeshaft, Phys. Rev. A **54**, 4299 (1996).
[24] M. Plummer and J. F. McCann, J. Phys. B **29**, 4625 (1996).
[25] M. Plummer and J. F. McCann, J. Phys. B **30**, L401 (1997).
[26] W.-C. Jiang, O. I. Tolstikhin, L.-Y. Peng, and Q. Gong, Phys. Rev. A **85**, 023404 (2012).
[27] O. I. Tolstikhin and H. Nakamura, J. Chem. Phys. **108**, 8899 (1998).
[28] O. I. Tolstikhin, V. N. Ostrovsky, and H. Nakamura, Phys. Rev. A **63**, 042707 (2001).
[29] D. Kato and S. Watanabe, Phys. Rev. A **56**, 3687 (1997).
[30] O. I. Tolstikhin, V. N. Ostrovsky, and H. Nakamura, Phys. Rev. Lett. **80**, 41 (1998).
[31] O. I. Tolstikhin and C. Namba, Phys. Rev. A **60**, 5111 (1999).
[32] O. I. Tolstikhin and C. Namba, *CTBC—A Program to Solve the Collinear Three-Body Coulomb Problem: Bound States and Scattering Below the Three-Body Disintegration Threshold*, *Research Report NIFS-779* (National Institute for Fusion Science, Toki, Japan, 2003) available at: [http://www.nifs.ac.jp/report/nifs779.html].
[33] C.-N. Liu, A.-T. Le, T. Morishita, B. D. Esry, and C. D. Lin, Phys. Rev. A **67**, 052705 (2003).
[34] O. I. Tolstikhin and C. Namba, Phys. Rev. A **70**, 062721 (2004).
[35] J. T. Muckerman, Chem. Phys. Lett. **173**, 200 (1990).
[36] C. Bloch, Nucl. Phys. **4**, 503 (1957).
[37] H. Miyagi, T. Morishita, and S. Watanabe, Phys. Rev. A **85**, 022708 (2012).
[38] E. P. Wigner and L. Eisenbud, Phys. Rev. **72**, 29 (1947).
[39] W. H. Press, S. A. Teukolsky, W. T. Vetterling, and B. P. Flannery, *Numerical Recipes in FORTRAN* (Cambridge University Press, Cambridge, 1992).
[40] G. Lagmago Kamta and A. D. Bandrauk, Phys. Rev. A **74**, 033415 (2006).